Semiconductors, Vol. 39, No. 5, 2005, pp. 528–532. Translated from Fizika i Tekhnika Poluprovodnikov, Vol. 39, No. 5, 2005, pp. 557–562.
Original Russian Text Copyright © 2005 by Bagraev, Klyachkin, Malyarenko, Ryskin, Shcheulin.

SEMICONDUCTOR STRUCTURES, INTERFACES, AND SURFACES

p^+-Si–n-CdF$_2$ Heterojunctions

N. T. Bagraev*^, L. E. Klyachkin*, A. M. Malyarenko*, A. I. Ryskin, and A. S. Shcheulin****
**Ioffe Physicotechnical Institute, Russian Academy of Sciences, Politekhnicheskaya ul. 26, St. Petersburg, 194021 Russia*
^e-mail: impurity.dipole@mail.ioffe.ru
***Vavilov State Optical Institute, Birzhevaya liniya 12, St. Petersburg, 199034 Russia*

Submitted November 4, 2004; accepted for publication November 25, 2004

Abstract—Boron diffusion and the vapor-phase deposition of silicon layers are used to prepare ultrashallow p^+–n junctions and p^+-Si–n-CdF$_2$ heterostructures on an n-CdF$_2$ crystal surface. Forward portions of the *I*–*V* characteristics of the p^+–n junctions and p^+-Si–n-CdF$_2$ heterojunctions reveal the CdF$_2$ band gap (7.8 eV), as well as allow the identification of the valence-band structure of cadmium fluoride crystals. Under conditions in which forward bias is applied to the p^+-Si–n-CdF$_2$ heterojunctions, electroluminescence spectra are measured for the first time in the visible spectral region. *© 2005 Pleiades Publishing, Inc.*

1. INTRODUCTION

The production of wide-gap semiconductor materials and heterostructures for developing emitters and photodetectors in wide ultraviolet and visible spectral ranges, as well as high-speed logic units for computer facilities and next-generation displays, is an important area of semiconductor nanoelectronics and optoelectronics. A promising wide-gap semiconductor for these purposes is cadmium fluoride (CdF$_2$), whose band gap (7.8 eV) is wider than that of diamond by a factor of 1.5 [1–5]. Nevertheless, despite the technology's simplicity and reproducibility, crystalline CdF$_2$ has remained, until recently, out of view of semiconductor physics due to its unipolar (n-type) conductivity. In this study, the possibility of overcoming this restriction using boron diffusion is shown for the first time. This process allows the production of ultrashallow p^+–n junctions on the n-CdF$_2$ crystal surface. Boron diffusion is also used to produce p^+-Si–n-CdF$_2$ heterostructures under the conditions of vapor-phase polysilicon deposition onto the n-CdF$_2$ crystal surface, which is facilitated by the close lattice constants of silicon and cadmium fluoride (5.43 and 5.46 Å, respectively) and their identical electron affinities (4 eV) [1–5].

2. EXPERIMENTAL

Ultrashallow p^+–n junctions on the surface of an n-CdF$_2$ crystal 1.0 mm thick were prepared by vapor-phase doping with boron. Since CdF$_2$ crystals are wide-gap insulators, n-type conductivity is attained by preliminary doping with Group III impurities, e.g., yttrium, gallium, or indium, followed by thermochemical coloration [6, 7]. It should be noted that this introduction of Group III impurities is not sufficient for producing n-type conductivity, since shallow donors are compensated by excess interstitial fluorine atoms.

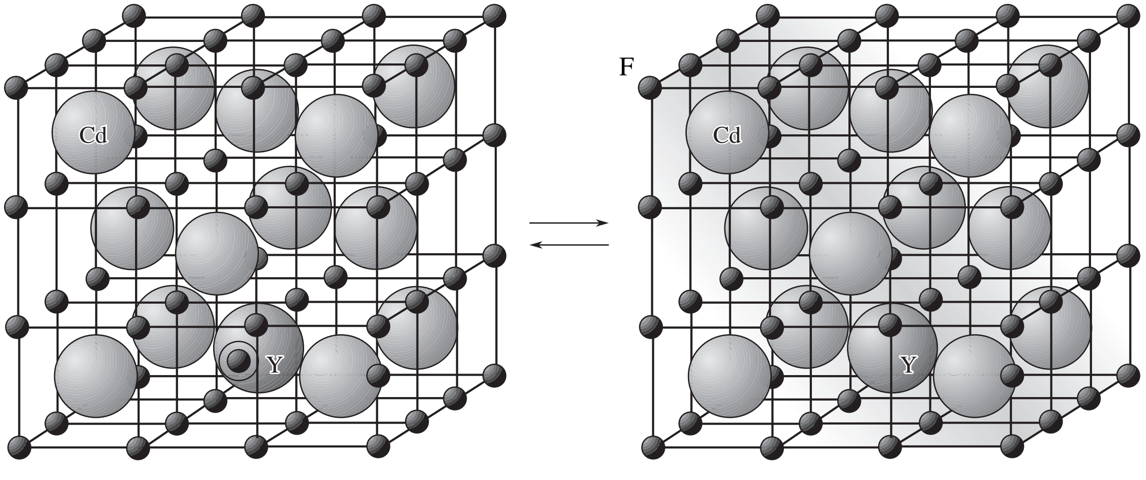

Fig. 1. The crystallographic structure of CdF$_2$. The arrows relate to thermochemical coloration and the subsequent by decoloration due to yttrium donor centers, which are accompanied by the removal and arrival of excess fluorine atoms, respectively.

1063-7826/05/3905-0528$26.00 © 2005 Pleiades Publishing, Inc.

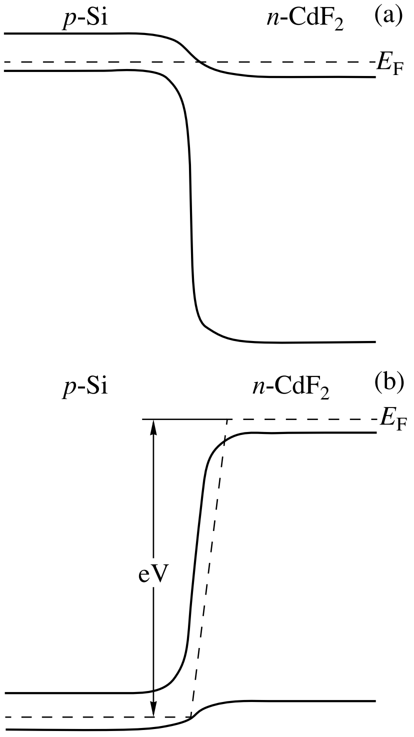

Fig. 2. A band diagram of the p^+-Si–n-CdF$_2$ heterojunction at zero (a) and forward (b) biases.

Therefore, further thermochemical treatment in a reduction atmosphere of metal vapor or hydrogen is required to remove these atoms, which results in crystal coloration due to local donor levels arising in the CdF$_2$ band gap (Fig. 1).

One of the optimum ways to achieve the p-type conductivity of CdF$_2$ crystals seems to be the substitution of lattice-site fluorine with boron, which, in this study, was carried out using vapor-phase boron diffusion. We note that a partial decoloration of the n-CdF$_2$ crystal during the doping with boron, accompanied by its transition to a semi-insulating state, was observed. Therefore, to restore the n-type conductivity of the CdF$_2$ crystal, additional thermochemical coloration was used after the vapor-phase doping. This technique made it possible to produce, for the first time, ultrashallow p^+ diffusion boron profiles at the surface of an n-CdF$_2$ crystal.

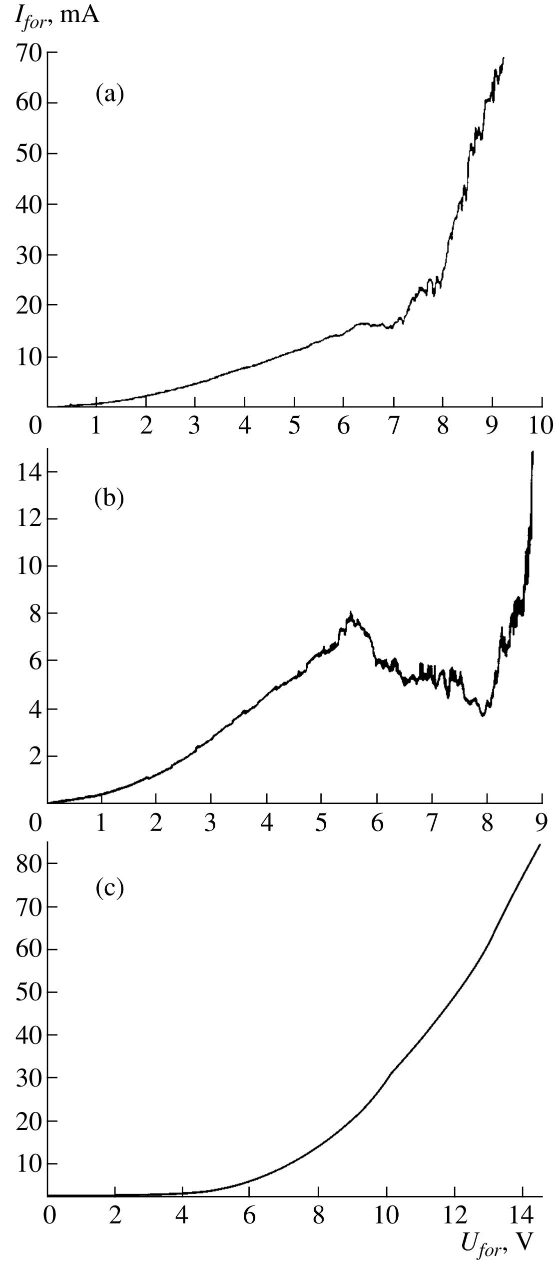

Fig. 3. Forward portions of the I–V characteristic of the p^+–n junction on (a) the CdF$_2$ surface and (b, c) p^+-Si–n-CdF$_2$ heterojunctions at $T = 300$ (a, b) and 77 K (c).

The p^+-Si–n-CdF$_2$ heterostructures were produced by the vapor-phase deposition of boron-doped silicon layers on the n-CdF$_2$ crystal surface. Variation in the deposition time made it possible to grow silicon layers 0.1–0.25 μm thick. The deposition temperature depended on the hydrogen and nitrogen contents in the chamber. It was found that thermally colored CdF$_2$ crystals were annealed during the deposition of p-type silicon layers, as in the case of vapor-phase doping with boron. This process transformed the crystals from the n-type conductivity to a semi-insulating state. Therefore, the above-described additional thermochemical coloration of the produced structures was carried out, which led to the CdF$_2$ crystals being transformed from the intrinsic conductivity into the n-type state. The above-listed sequential operations allowed the production of p^+-Si–n-CdF$_2$ heterostructures (Fig. 2a) for the first time.

Contacts to the boron-doped n-CdF$_2$ crystal surface and heavily boron-doped silicon layers grown by vapor-phase deposition were formed using gold deposition. A study of the I–V characteristics showed that the surface barriers were almost completely absent in the ohmic contacts [8]. Contacts to the rear surface of the n-CdF$_2$ crystal were formed by a low-temperature

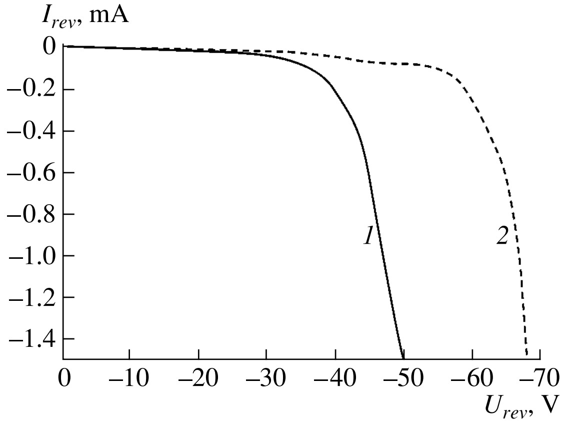

Fig. 4. Reverse portions of the *I–V* characteristic of the p^+-Si–n-CdF$_2$ heterojunctions grown by the vapor-phase deposition of doped polycrystalline silicon onto (*1*) weakly and (*2*) strongly colored cadmium fluoride substrates.

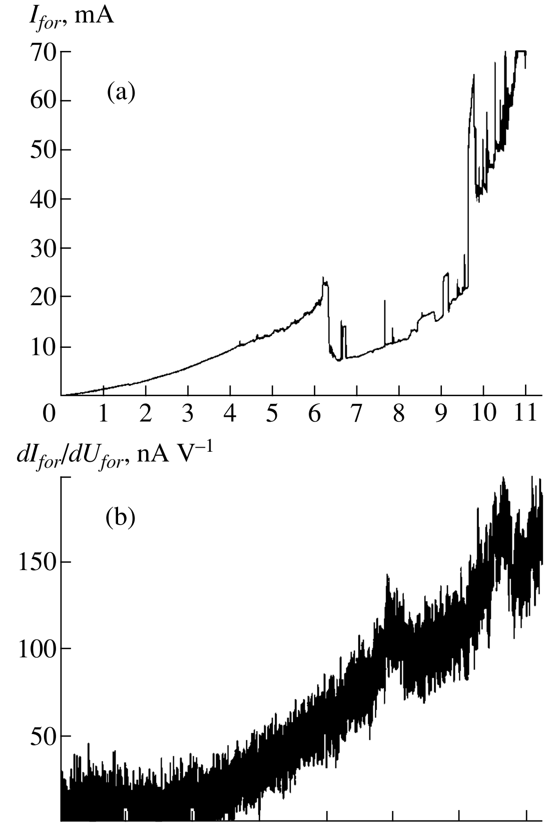

Fig. 5. Forward portions of the *I–V* characteristic of the p^+-Si–n-CdF$_2$ heterojunction, measured after a preliminary exposure to light in the IR wavelength range (1–27 μm), which demonstrate the structure of the CdF$_2$ valence band. T = 300 (a) and 77 K (b).

vapor-phase deposition of ytterbium silicide. The existence of p^+–n junctions on the CdF$_2$ surface and p^+-Si–n-CdF$_2$ heterojunctions was revealed by analyzing the *I–V* characteristics (Figs. 3a, 3b). The forward portions of the *I–V* characteristics are indicative of the existence of the CdF$_2$ band gap (7.8 eV), which controls the formation of the p^+–n junction and heterojunction. The stability of the electrical characteristics of the produced p^+–n junctions and heterojunctions was studied in relation to the temperature and duration of the vapor-phase doping and deposition, as well as the atmosphere composition (vacuum, argon, and nitrogen). It was found that pronounced thermal coloration of n-CdF$_2$, in comparison to weakly pronounced coloration, results in the lowest leakage current of the grown structures (Fig. 4).

3. RESULTS AND DISCUSSION

Not only are the forward portions of the *I–V* characteristics of p^+-Si–n-CdF$_2$ heterojunctions indicative of the CdF$_2$ band gap (7.8 eV), but they also exhibit a region of negative differential resistivity (Fig. 3b). The latter is apparently caused by a decrease in the probability of hole tunneling from the silicon valence band to the CdF$_2$ conduction band as the forward voltage increases (Fig. 2b). This assumption is confirmed by a change in the shape of the *I–V* characteristic as the temperature decreases, which demonstrates the suppression of the negative differential resistivity due to electron freezing at the donor levels in n-CdF$_2$ (Fig. 3c).

The use of preliminary exposure to light in the IR wavelength range (1–27 μm) made it possible to increase the slope of the negative differential resistivity, which is associated with ionization of the shallow donors in the n-CdF$_2$ crystal (Fig. 5a) [4, 5]. Furthermore, the photoionization of the shallow donors results in a sharp increase in the current at a forward bias due to an increase in the lifetime of the injected holes passing through the 1.0-mm-thick CdF$_2$ crystal (Fig. 5a). As a result of this increase in p-type conductivity and the identical electron affinities of silicon and cadmium fluoride (4 eV) [8], the study of the forward portions of the *I–V* characteristic made it possible to determine the valence band structure of the CdF$_2$ crystal (Figs. 5a, 5b).

The measured high-resolution *I–V* characteristics are consistent with the calculated energy structure of the valence band of cadmium fluoride [9–11], as well as with the density of states in this band, determined using optical [12] and photoelectron spectroscopy [13–15] (Fig. 6). In particular, the excitonic peak and direct transitions Γ_{15}–Γ_1 and Γ_{25}–Γ_1 manifest themselves at 7.87, 8.5, and 9.98 eV, respectively, whereas the X_5–Γ_1 transition occurs at 8.05 eV. Despite the fact that the excitonic peak is observed at somewhat higher energies than could be expected from the data of optical measurements and photoelectron spectroscopy [12, 14], the results obtained are consistent with the polaron model if the measured Γ_{15}–Γ_1 energies are taken into account.

The peaks at 9.78, 10.12, and 10.19 eV are apparently caused by the contribution of the L_3, L_2, and L_1

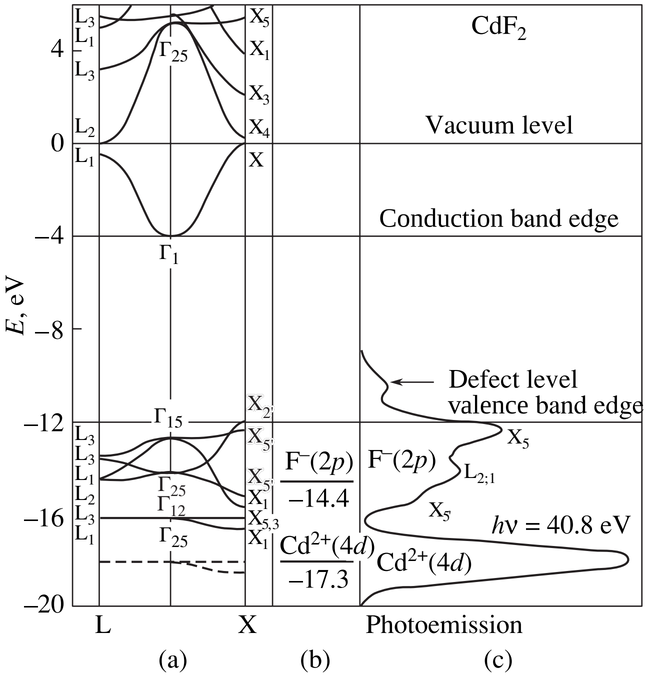

Fig. 6. A band diagram of the cadmium fluoride crystal [13]: (a, b) states of the CdF$_2$ valence band and (c) the density of states according to the photoemission measurement data [13].

states of the CdF$_2$ valence band, while the transitions arising due to the X$_5$ and X$_1$ states of the CdF$_2$ valence band are resolved in the energy range 10.9–11.2 eV. In turn, Cd^{2+}(4d) states are observed at the forward biases of 13.27 and 13.75 eV (Fig. 5b). The observed d-state splitting is probably due to spin–orbit splitting or splitting induced by the crystal field [12, 14, 15].

The feasibility of tunnel spectroscopy in relation to the CdF$_2$ valence band in the produced heterojunctions and p^+–n junctions is apparently indicative of a ballistic transport mechanism for the holes injected into n-CdF$_2$. To determine the parameters of this hole transport, we studied the I–V characteristics over the p^+–n junction plane and Si–CdF$_2$ interface. The measurements yielded an unexpected result: the metal conductivity of quasi-two-dimensional hole gas (Fig. 7). These data indicate the formation of a two-dimensional layer, whose properties are close to those of a hypothetical CdB$_2$ compound, which should apparently feature p-type conductivity. Quasi-one-dimensional fluctuations of this compound toward n-CdF$_2$ promote the formation of short quantum wires, along which the electric field is localized as a forward voltage is applied. This effect is responsible for the induction of the ballistic transport of holes in the naturally formed anionic sublattice (Fig. 8). Hole tunneling into the valence band of cadmium fluoride through a two-dimensional metal depends on the band structure of the latter, which results in peaks at 6.84 and 6.92 eV in the forward portion of the I–V characteristic at energies lower than the CdF$_2$ band gap (Fig. 5a).

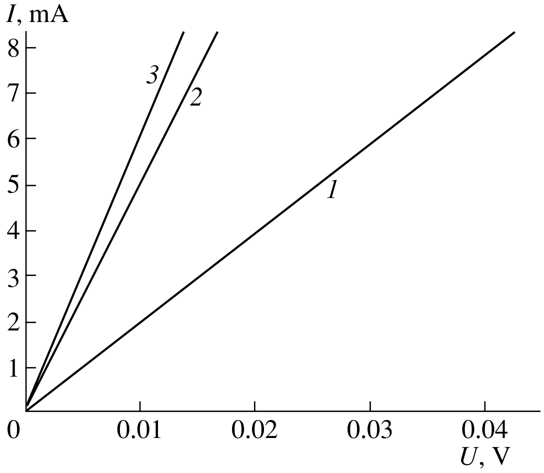

Fig. 7. I–V characteristics in the p^+–n junction plane on the n-CdF$_2$ surface at (1) 300, (2) 77, and (3) 4.2 K.

Studies of the photoluminescence and electroluminescence of the produced p^+-Si–n-CdF$_2$ heterojunctions in the infrared spectral region, carried out using an IFS-115 IR Fourier spectrometer, indicated the formation of microcavities embedded into the system of self-assembled silicon nanostructures that form the p^+-Si layer deposited from the vapor phase. Under the conditions in which a forward bias is applied to the produced p^+-Si–n-CdF$_2$ heterojunctions, the electroluminescence spectra in the visible wavelength region were measured for the first time (Fig. 9). These spectra arise due to radiative recombination of the holes and electrons injected at the Si–CdF$_2$ interface.

4. CONCLUSION

Ultrashallow p^+–n junctions on the surface of n-CdF$_2$ crystals and p^+-Si–n-CdF$_2$ heterostructures were produced using boron diffusion and the vapor-phase deposition of silicon layers onto the n-CdF$_2$ surface. It is shown that thermally colored CdF$_2$ crystals were annealed during vapor-phase doping and deposition, which transformed them from n-type conductivity into a semi-insulating state. Due to a subsequent coloration, CdF$_2$ crystals were again transformed from the intrinsic conductivity into n-type conductivity.

The study of the reverse and forward portions of the I–V characteristics made it possible to establish the formation of ohmic contacts on the surface of heavily doped p-type silicon layers and n-CdF$_2$, which exhibit an almost total absence of surface barriers.

The forward portions of the I–V characteristics of the p^+–n junctions and p^+-Si–n-CdF$_2$ heterojunctions indicate the presence of the CdF$_2$ band gap (7.8 eV). The I–V characteristics of the p^+-Si–n-CdF$_2$ heterojunctions also exhibit a region of negative differential resistivity, which is caused by the existence of a degenerate hole gas at the Si–CdF$_2$ interface.

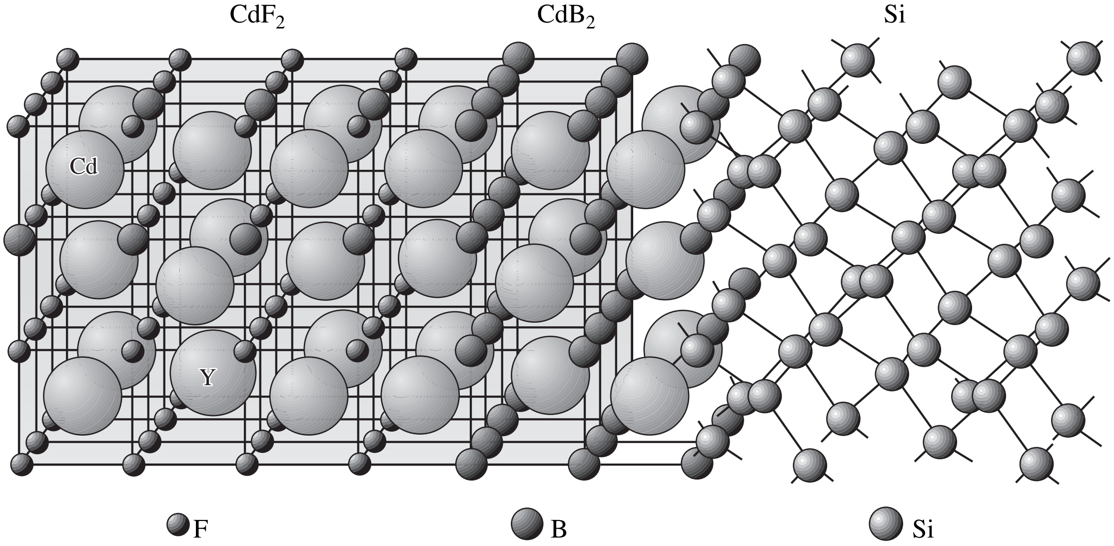

Fig. 8. The structure of the p^+-Si–n-CdF_2 heterojunction with a two-dimensional CdB_2 layer, whose fluctuations penetrate into n-CdF_2.

The study of the forward portions of the *I*–*V* characteristics of the p^+–n junctions and p^+-Si–n-CdF_2 heterojunctions made it possible to clarify the valence-band structure of cadmium fluoride crystals, which seems to manifest itself due to the ballistic transport of holes injected in the n-CdF_2 volume. The observed high-resolution *I*–*V* characteristic is in good agreement with the data on the CdF_2 valence-band structure, which were obtained using optical [12] and photoelectron [13–15] spectroscopy.

Under conditions in which a forward bias was applied to the grown p^+-Si–n-CdF_2 heterojunctions, electroluminescence spectra were measured in the visible wavelength region for the first time. This luminescence arises due to radiative recombination of the holes and electrons injected from the Si–CdF_2 interface.

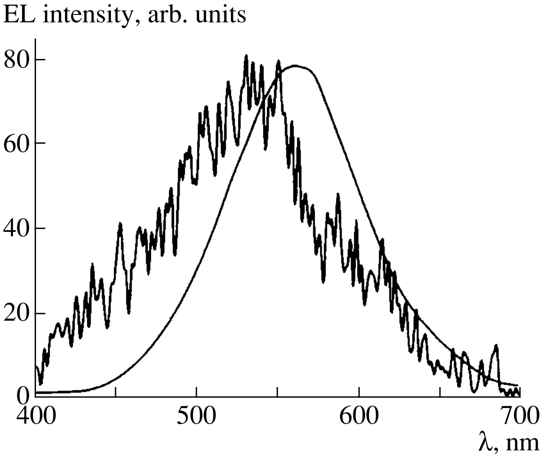

Fig. 9. The electroluminescence spectrum at a forward bias of the p^+-Si–n-CdF_2 heterojunction (the forward current is ~90 mA). The solid curve is the spectral characteristic of the human eye.

ACKNOWLEDGMENTS

This study was supported by the International Science and Technology Center, project no. 2136.

REFERENCES

1. F. Trautweiler, F. Moser, and R. P. Khosla, J. Phys. Chem. Solids **29**, 1869 (1968).
2. F. Moser, D. Matz, and S. Lyu, Phys. Rev. **182**, 808 (1969).
3. J. M. Langer, T. Langer, G. L. Pearson, *et al.*, Phys. Status Solidi B **66**, 537 (1974).
4. S. A. Kazanskii, D. S. Rumyantsev, and A. I. Ryskin, Phys. Rev. B **65**, 165214 (2002).
5. A. I. Ryskin, A. S. Shcheulin, B. Koziarska, *et al.*, Appl. Phys. Lett. **67**, 31 (1995).
6. J. D. Kingsley and J. S. Prener, Phys. Rev. Lett. **8**, 315 (1962).
7. J. S. Prener and J. D. Kingsley, J. Chem. Phys. **38**, 667 (1963).
8. J. Garbarczyk, B. Krukowska-Fulde, T. Langer, and J. M. Langer, J. Phys. D **11**, L17 (1978).
9. J. P. Albert, C. Jouanin, and G. Gout, Phys. Rev. B **16**, 4619 (1977).
10. N. V. Starostin and M. P. Shepilov, Fiz. Tverd. Tela (Leningrad) **17**, 822 (1975) [Sov. Phys. Solid State **17**, 523 (1975)].
11. V. K. Bashenov, I. Bauman, and V. V. Timofeenko, Phys. Status Solidi B **81**, K55 (1977).
12. C. Raisin, J. M. Berger, S. Robin-Kandare, *et al.*, J. Phys. C **13**, 1835 (1980).
13. B. A. Orlowdki and J. M. Langer, Acta Phys. Pol. A **63**, 107 (1983).
14. B. A. Orlowski and J. M. Langer, Phys. Status Solidi B **91**, K53 (1979).
15. R. T. Poole, J. A. Nicholson, J. Liesegang, *et al.*, Phys. Rev. B **20**, 1733 (1979).

Translated by A. Kazantsev